

The actuation equation of macro-fiber composite coupled plate and its active control over the vibration of plate and shell

Jianwei Tu^{*}, Jiarui Zhang^a, Qianying Zhu^b, Fan Liu^c and Wei Luo^d

Hubei Key Laboratory of Roadway Bridge and Structure Engineering, Wuhan University of Technology, 122 Luoshi Road Wuhan, China

(Received February 13, 2018, Revised March 13, 2018, Accepted March 23, 2018)

Abstract. Plate and shell structure is widely applied in engineering, i.e. building roofs, aircraft wings, ship platforms, and satellite solar arrays. Its vibration problem has become increasingly prominent due to the tendency of lightening, upsizing and flexibility. As a new smart material with great actuating force and toughness, macro-fiber composite (MFC) is composed of piezoelectric fiber and epoxy resin basal body, which can be directly pasted onto the surface of plate and shell and is suitable for vibration control. This paper deduces the actuation equation of MFC coupled plate in different boundary conditions, an equivalent finite element modeling method is proposed which uses MFC actuating force as the applied excitation, and on this basis the active control simulation and experiment of MFC over plate and shell structure vibration are accomplished. The results indicate that MFC is able to implement effective control over plate and shell structure vibration in multi-band range. The comparison between experiment and simulation proves that the actuation equation deduced herein, effective and practicable, can be applied into the simulation calculation of MFC vibration control over plate and shell structure.

Keywords: plate and shell structure; macro-fiber composite; actuation equation; active control

1. Introduction

Piezoelectric material is one of the most widely-used smart materials. Sensing and driving can be implemented by its direct piezoelectric effect and inverse piezoelectric effect. Piezoelectric ceramics is often used at present, but it cannot be used in curved surface structures due to its weak piezoelectric effect, fragile texture, and poor flexibility. To overcome those defects, NASA has developed a new piezoelectric composite – macro fiber composite (MFC), which is composed of piezoelectric ceramics fiber, epoxy resin basal body, and interdigitated electrodes. Compared with traditional piezoelectric ceramics, the protection of resin basal body greatly overcomes the defects of strength and fragility, and the fiber tremendously improves flexibility and piezoelectric effect of the material (2002). By applying voltage to MFC, its inverse piezoelectric effect is used to make

^{*}Corresponding author, Professor, E-mail: tujianwei@whut.edu.cn

^aMaster student, E-mail: ZJR1207916099@outlook.com

^bMaster student, E-mail: 502027514@qq.com

^cMaster student, E-mail: 1044643049@qq.com

^dMaster student, E-mail: 769587515@qq.com

an actuator to carry out active control over the structure vibration. If the structure deformation produced by external excitation is contrary to that by MFC, they offset each other and thereby reduce the structure vibration and noise.

In studying MFC active control over structural vibration, establishing the mechanical model of MFC actuator is significant. In the aspect of mechanical properties of MFC material, Zhao *et al.* (2014) verified this modeling method by making the numerical simulation about MFC electromechanical properties with ABAQUS finite element software and comparing them with the experimental results. On the basis of plane stress hypothesis, Deraemaeker *et al.* (2009) established MFC mechanical model by mixing rules with uniform field method and studied the influence of volume fraction of piezoelectric ceramics fiber on MFC piezoelectric coefficient. On this basis, Prasath and Arockiarajan (2013, 2014), by using equivalent stratification and considering the influence of epoxy resin basal body and composite material, further studied the influence of volume fraction of piezoelectric ceramics fiber on MFC elastic modulus, piezoelectric coefficient, and stress-strain. Bilgen *et al.* (2010) proposed the establishment of the cantilever type of MFC mechanical model by electromechanical model with linearly distributed parameters and verified this modeling method by comparing the electrical poling vibration frequency derived by this model with the experiment. Steiger and Mokry (2015) approximated MFC to plate uniform piezoelectric material and on this basis established MFC finite element model to simplify the model.

Since MFC come into play only by pasting to the structure, the mechanical model of MFC coupled structure is needed and the study of MFC model provides theoretical basis for establishing the model of MFC coupled structure. With regard to MFC coupled beam, Zhang *et al.* (2015) established the finite element model with MFC composite cantilever beam by using linear piezoelectric constitutive equation based on Reissner-Mindlin theory, and studied the deformation degree of cantilever beam made by the different angle of MFC piezoelectric fiber under the given normal pressure. Aiming at the vibration made by the axial movement of cantilever beam, Ma *et al.* (2016) proposed that MFC could be used as the actuator to control its vibration and achieved a good controlling effect. They deduced the free vibration equation of beam axial movement by Hamilton principle and took MFC effect on the main structure as external controlling force.

The vibration problem of plate and shell structure has been increasingly prominent. In studying the mechanical model of MFC coupled plate, Yi *et al.* (2011) simplified the MFC constitutive equation into a two-dimensional one in mechanical model deduction. He ignored the deformation in through-thickness direction and established the vibration differential equation of MFC coupled plate based on two-dimensional constitutive relation. Sohn and Choi (2014) studied the vibration of the cylinder which is attached to MFC, deduced the mechanical model of the ship cylinder structure which is attached to MFC with Donnell-Mushtari theory and Lagrange equation, and implemented active control over the cylinder with genetic algorithm. On the basis of the theory of first-order shear deformation, Kumar *et al.* (2012) established MFC mechanical model by using the four-node composite plate-shell unit with warpage which can further modify out-of-plane distortion and simulate the shell deformation characteristics better. Based on Donnell-Mushtari shell theory, Kwak *et al.* (2009) established the mechanical model of cylinder shell attached to MFC actuator and sensor with Rayleigh-Ritz method. In MFC mechanical model, he applied pin-force model to establish MFC actuating force formula, believing MFC provides the structure with equivalent applied force. This simplified formula only considers three factors – MFC piezoelectric coefficient d_{33} , elastic modulus, and applied potential gradient. Kim *et al.* (2011) studied the active control of vibration over the cantilever cylinder shell attached to MFC. In terms

of the mechanical model of MFC coupled plate, he took the MFC influence on the main structure as equivalent force and equivalent moment of force and imposed them onto the structure.

Those researches show that various mechanical models derivation of MFC coupled structures assume the internal force of the coupled structure is zero, that is the boundary condition of the structure is free. Yet, the internal force dose exist in the actual structure under load when its boundary condition is under restriction, and this force has an effect on MFC action. Accordingly, this paper considers the influence of cross-section internal force at MFC paste position under the binding boundary condition on MFC actuating force and deduces the actuation equation of MFC coupled plate under the binding boundary condition. On this basis, the MFC active control simulation and experimental verification are accomplished over the plate and arcing shell structure vibration.

2. The actuation equation of MFC coupled plate

2.1 The piezoelectric equation of MFC material

The homogeneous active layer of MFC can be viewed as piezoelectric ceramics, as is shown in Fig. 1. The stress-strain equation of MFC linear elastic piezoelectric material polarized in the x direction is written as

$$\begin{bmatrix} \varepsilon_z \\ \varepsilon_y \\ \varepsilon_x \\ \gamma_{yx} \\ \gamma_{xz} \\ \gamma_{zy} \end{bmatrix} = \begin{bmatrix} s_{11}^E & s_{12}^E & s_{13}^E & 0 & 0 & 0 \\ s_{21}^E & s_{22}^E & s_{23}^E & 0 & 0 & 0 \\ s_{31}^E & s_{32}^E & s_{33}^E & 0 & 0 & 0 \\ 0 & 0 & 0 & s_{44}^E & 0 & 0 \\ 0 & 0 & 0 & 0 & s_{55}^E & 0 \\ 0 & 0 & 0 & 0 & 0 & s_{66}^E \end{bmatrix} \begin{bmatrix} \sigma_z \\ \sigma_y \\ \sigma_x \\ \tau_{yx} \\ \tau_{xz} \\ \tau_{zy} \end{bmatrix} + \begin{bmatrix} 0 & 0 & d_{31} \\ 0 & 0 & d_{32} \\ 0 & 0 & d_{33} \\ 0 & d_{24} & 0 \\ d_{15} & 0 & 0 \\ 0 & 0 & 0 \end{bmatrix} \begin{bmatrix} 0 \\ 0 \\ E_x \end{bmatrix} \quad (1)$$

In which, s_{ij}^E is flexibility coefficient; d_{ij} is piezoelectric strain coefficient; E_x is the electric field intensity in the x direction.

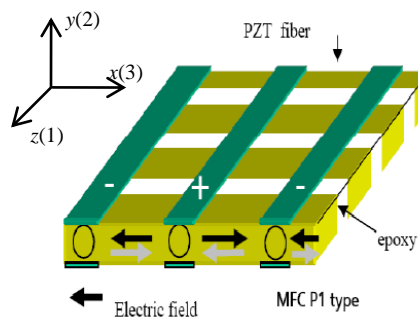


Fig. 1 MFC homogeneous active layer unit structure

MFC is in slice form, only 0.3mm thick. According to thin shells vibration theory, stress and strain in the y direction can be ignored. As a result, Eq. (1) is simplified into

$$\begin{bmatrix} \varepsilon_z \\ \varepsilon_x \\ \gamma_{xz} \end{bmatrix} = \begin{bmatrix} s_{11}^E & s_{13}^E & 0 \\ s_{13}^E & s_{33}^E & 0 \\ 0 & 0 & s_{44}^E \end{bmatrix} \begin{bmatrix} \sigma_z \\ \sigma_x \\ \tau_{xz} \end{bmatrix} + \begin{bmatrix} 0 & 0 & d_{31} \\ 0 & 0 & d_{33} \\ d_{15} & 0 & 0 \end{bmatrix} \begin{bmatrix} 0 \\ 0 \\ E_x \end{bmatrix} \quad (2)$$

It is observed from Eq. (2) that the shear strain γ_{xz} of MFC has nothing to do with electric field intensity E_x , and the shear strain τ_{xz} of MFC itself is too small that its influence can be ignored. Eq. (2) is further simplified into

$$\begin{bmatrix} \varepsilon_z \\ \varepsilon_x \end{bmatrix} = \begin{bmatrix} s_{11}^E & s_{13}^E \\ s_{13}^E & s_{33}^E \end{bmatrix} \begin{bmatrix} \sigma_z \\ \sigma_x \end{bmatrix} + \begin{bmatrix} d_{31} \\ d_{33} \end{bmatrix} E_x \quad (3)$$

The electric field intensity E_x inside MFC is

$$E_x = \frac{V}{w_{pitch}} \quad (4)$$

in which V is the applied voltage amplitude and w_{pitch} is the interpolation electrode spacing of MFC wire electrodes.

2.2 The actuation equation of MFC coupled plate

2.2.1 The actuation equation of MFC coupled plate under free boundary condition

The two-dimensional MFC coupled plate is depicted by the plate theory, as is shown in Fig. 2. The plate thickness is H ; the effective length of MFC is a , width b , and thickness h ; L is the distance between the neutral axis and the surface of the plate.

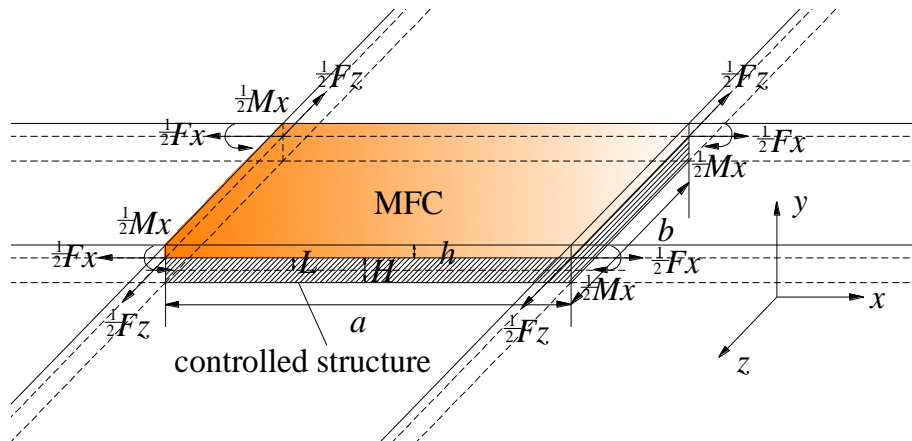


Fig. 2 the unit structure of MFC coupled plate

From Eq. (3), the stress of the two-dimensional MFC coupled plate is

$$\begin{bmatrix} \sigma_z \\ \sigma_x \end{bmatrix} = \begin{bmatrix} Q_{11}^E & Q_{13}^E \\ Q_{31}^E & Q_{33}^E \end{bmatrix} \begin{bmatrix} \varepsilon_z - d_{31}E_x \\ \varepsilon_x - d_{33}E_x \end{bmatrix} \quad (5)$$

in which matrix Q^E is the inverse matrix of matrix s^E

$$Q_{11}^E = \frac{s_{33}^E}{s_{11}^E s_{33}^E - (s_{13}^E)^2}, Q_{13}^E = Q_{31}^E = \frac{-s_{13}^E}{s_{11}^E s_{33}^E - (s_{13}^E)^2}, Q_{33}^E = \frac{s_{11}^E}{s_{11}^E s_{33}^E - (s_{13}^E)^2} \quad (6)$$

The two-dimensional flexibility matrix is written as

$$\begin{bmatrix} s_{11}^E & s_{13}^E \\ s_{31}^E & s_{33}^E \end{bmatrix} = \begin{bmatrix} \frac{1}{E_s} & \frac{-\mu_s}{E_s} \\ \frac{-\mu_s}{E_s} & \frac{1}{E_s} \end{bmatrix} \quad (7)$$

in which μ_s is the Poisson ratio of MFC.

Under free boundary condition, the MFC actuating bending moment to the two-dimensional plate is

$$\begin{cases} M_z = a \int_L^{L+h} (-\sigma_z) y dy = a \int_L^{L+h} [Q_{11}^E (d_{31}E_x - \varepsilon_z) + Q_{13}^E (d_{33}E_x - \varepsilon_x)] y dy \\ M_x = b \int_L^{L+h} (-\sigma_x) y dy = b \int_L^{L+h} [Q_{31}^E (d_{31}E_x - \varepsilon_z) + Q_{33}^E (d_{33}E_x - \varepsilon_x)] y dy \end{cases} \quad (8)$$

According to bending deformation theory, the bending strain of the two-dimensional MFC coupled plate is

$$\begin{bmatrix} \varepsilon_z \\ \varepsilon_x \end{bmatrix} = \begin{bmatrix} \frac{y}{\rho_z} \\ \frac{y}{\rho_x} \end{bmatrix} \quad (9)$$

in which ρ_x, ρ_z are respectively the bending radius of the two-dimensional MFC coupled plate along the x, z directions.

According to the bending deformation theory, curvature radius ρ is

$$\begin{cases} \rho_x = \frac{E_p I_{px}}{M_x} \\ \rho_z = \frac{E_p I_{pz}}{M_z} \end{cases} \quad (10)$$

in which I_{px}, I_{pz} are respectively the x axis inertia moment and the z axis inertia moment of the plate cross-section.

MFC thickness h is quite small. Eqs. (9) and (10) are substituted into Eq. (8) so that the actuating moment is obtained

$$\begin{cases} M_z = \frac{a(1+D)(Q_{11}^E d_{31} + Q_{13}^E d_{33}) - bB(Q_{31}^E d_{31} + Q_{33}^E d_{33})}{(1+A)(1+D) - BC} LhE_x \\ M_x = \frac{b(1+A)(Q_{31}^E d_{31} + Q_{33}^E d_{33}) - aC(Q_{11}^E d_{31} + Q_{13}^E d_{33})}{(1+A)(1+D) - BC} LhE_x \end{cases} \quad (11)$$

in which

$$\begin{aligned} A &= \frac{aQ_{11}^E}{E_p I_{pz}} L^2 h, B = \frac{aQ_{13}^E}{E_p I_{px}} L^2 h \\ C &= \frac{bQ_{31}^E}{E_p I_{pz}} L^2 h, D = \frac{bQ_{33}^E}{E_p I_{px}} L^2 h \end{aligned} \quad (12)$$

MFC actuating force to the two-dimensional plate is

$$\begin{cases} F_z = a \int_L^{L+h} (-\sigma_z) dy = a \int_L^{L+h} [Q_{11}^E (d_{31} E_x - \varepsilon_z) + Q_{13}^E (d_{33} E_x - \varepsilon_x)] dy \\ F_x = b \int_L^{L+h} (-\sigma_x) dy = b \int_L^{L+h} [Q_{31}^E (d_{31} E_x - \varepsilon_z) + Q_{33}^E (d_{33} E_x - \varepsilon_x)] dy \end{cases} \quad (13)$$

Eq. (13) can also be simplified as the following because of the small thickness

$$\begin{cases} F_z = \frac{a(1+D)(Q_{11}^E d_{31} + Q_{13}^E d_{33}) - bB(Q_{31}^E d_{31} + Q_{33}^E d_{33})}{(1+A)(1+D) - BC} hE_x \\ F_x = \frac{b(1+A)(Q_{31}^E d_{31} + Q_{33}^E d_{33}) - aC(Q_{11}^E d_{31} + Q_{13}^E d_{33})}{(1+A)(1+D) - BC} hE_x \end{cases} \quad (14)$$

2.2.2 The actuation equation of MFC coupled plate under the binding boundary condition

The internal force of plate structures under the free boundary condition in MFC actuating field is zero. Yet the actual structure is under the binding boundary condition, namely, the internal force is not zero. Therefore, this internal force produces influence on MFC actions on the plate.

After the internal force exists in the structure, Eq. (10) is

$$\begin{cases} \rho_x = \frac{E_p I_{px}}{M_x + M_{x0}} \\ \rho_z = \frac{E_p I_{pz}}{M_z + M_{z0}} \end{cases} \quad (15)$$

in which M_{x0} , M_{z0} are respectively the bending moments made by cross-section stress at the MFC paste position under the binding boundary condition;

By substituting Eqs. (10)-(15) into Eq. (8), MFC driving moment under the binding boundary condition is obtained

$$\left\{ \begin{array}{l} M_x = \frac{bh \left(9FE_x J (d_{31}Q_{31}^E + d_{33}Q_{33}^E) + 2ahH^2 M_{x0} G \right.}{2(9F + 3E_p hHK)} \\ \left. - 3E_p H (2I_{pz} M_{x0} Q_{33}^E + I_{px} (2M_{z0} Q_{31}^E + ad_{33} E_x hJG)) \right) \\ M_z = \frac{ah \left(9d_{33} FE_x J Q_{13}^E - 6E_p H (I_{px} M_{z0} Q_{11}^E + I_{pz} M_{x0} Q_{13}^E) \right.}{2(9F + 3E_p hHK)} \\ \left. + 2bhH^2 M_{z0} G + 3d_{31} E_p E_x I_{pz} J (3E_p I_{px} Q_{11}^E - bhHG) \right) \end{array} \right. \quad (16)$$

in which

$$\begin{aligned} F &= E_p^2 I_{px} I_{pz}, G = Q_{13}^E Q_{31}^E - Q_{11}^E Q_{33}^E \\ H &= h^2 + 3hL + 3L^2, J = h + 2L \\ K &= aI_{px} Q_{11}^E + bI_{pz} Q_{33}^E \end{aligned} \quad (17)$$

Under the binding boundary condition, the MFC actuating force to the two-dimensional plate structure is

$$\left\{ \begin{array}{l} F_x = \frac{bh \left(36d_{33} FE_x Q_{33}^E + 6ahGHJM_{x0} \right.}{4(9F + 3E_p hHK)} \\ \left. + 3E_p \left(-3I_{px} J (2M_{z0} + ad_{33} E_x hJQ_{13}^E) Q_{31}^E \right. \right. \\ \left. \left. + 2(-3I_{pz} JM_{x0} + 2ad_{33} E_x hI_{px} HQ_{11}^E) Q_{33}^E \right) + 36Fd_{31} E_x Q_{31}^E \right) \\ F_z = \frac{ah \left(36d_{33} FE_x Q_{13}^E - 6bhGHJM_{z0} - 18E_p J (I_{px} M_{z0} Q_{11}^E + I_{pz} M_{x0} Q_{13}^E) \right.}{4(9F + 3E_p hHK)} \\ \left. + d_{31} E_x (36FQ_{11}^E + 3bhE_p I_{pz} (-3J^2 Q_{13}^E Q_{31}^E + 4HQ_{11}^E Q_{33}^E)) \right) \end{array} \right. \quad (18)$$

Eqs. (16)-(18) are applicable to the actuating force calculation of MFC in the plate and shell structure under the binding boundary condition, and the determination of M_{x0} , M_{z0} depends on the boundary condition of the plate and shell structure.

3. The active control of MFC over plate and shell vibration

The active control equation of simple structures can be obtained by analytic method. However, actual structures are normally very complicated rather than regular and simple. Thus, on the basis of a universe actuating equation of MFC coupled plate, a finite element modeling method is proposed that MFC is viewed as external excitation to deduce the active control equation of the structure. SHELL63 unit is chosen to establish the model of the plate and shell structure. Since the elastic modulus of the plate structure is much greater than that of MFC, MFC basically has no

influence on the dynamic characteristic of plate and shell. In modeling, the actuating force and bending moment of MFC are imposed onto the plate and shell structure in the form of external force. In finite element modeling, the controlling force of the finite element model should be calibrated to obtain the position matrix of the controlling force. Then according to the mass matrix, stiffness matrix, and the position matrix of the controlling force from finite element, the dynamical equations are established to obtain the state space equations of the plate structure under control

$$\begin{cases} M \{\ddot{x}\} + D \{\dot{x}\} + K \{x\} = B_{01}F + B_{02}U \\ y = C_{oq}x + C_{ov}\dot{x} \end{cases} \quad (19)$$

in which M , D , K are mass, damping and stiffness matrixes of the plate and shell structure, F the external exciting force, B_{01} the position matrix of the exciting force, U the controlling force made by MFC, B_{02} position matrix of the controlling force, C_{oq} displacement output matrix, and C_{ov} speed output matrix.

State variable is defined as

$$q = \begin{Bmatrix} q_1 \\ q_2 \end{Bmatrix} = \begin{Bmatrix} x \\ \dot{x} \end{Bmatrix} \quad (20)$$

Then Eq. (19) can be described as state space

$$\begin{cases} \dot{q} = Aq + B_1F + B_2U \\ y = Cq \end{cases} \quad (21)$$

in which

$$A = \begin{bmatrix} 0 & I \\ -KM^{-1} & -M^{-1}D \end{bmatrix}_{2n \times 2n}, B_1 = \begin{bmatrix} 0 \\ M^{-1}B_{01} \end{bmatrix}, B_2 = \begin{bmatrix} 0 \\ M^{-1}B_{02} \end{bmatrix}, C = [C_{oq} \ C_{ov}]_{1 \times 2n} \quad (22)$$

$$B_{01} = \begin{bmatrix} 0 \\ 0 \\ \vdots \\ 0 \\ b_{11} \\ 0 \\ \vdots \\ 0 \end{bmatrix}_{2n \times 1}, B_{02} = \begin{bmatrix} 0 \\ 0 \\ \vdots \\ 0 \\ b_{21} \\ b_{22} \\ \vdots \\ 0 \end{bmatrix}_{2n \times 1}, C_{oq} = [0 \ \cdots \ 1]_{1 \times n}, C_{ov} = [0 \ \cdots \ 0]_{1 \times n} \quad (23)$$

in which n is freedom degree of the structure, b_{11} , b_{21} , $b_{22} \cdots$ are the controlling force or moment produced by 1V voltage at the nodes attached to MFC respectively, which is calculated by Eqs. (16)-(18).

4. Simulation analysis

Vibration response of plate and shell structure attached to MFC is simulated. The structures area flat plate and an arc shell, whose parameters are shown in Table 1. The M8514-P1 type of MFC is chosen to simulate the vibration control, and its parameters are in Table 2. In simulation analysis, excitation force is a sinusoidal load of 100 N, which of 20 Hz and 50 Hz are exerted to the center position of plate and shell structure. The needed controlling voltage is obtained by PID control.

Table 1 parameters of the plate and shell structure

Material	Elastic Modulus	Density	Poisson Ratio	Width/Span	Width	Thickness	Hight
Flat Plate (Al)	70.5 GPa	2700 kg/m ³	0.30	400 mm	400 mm	2 mm	\
Arc Shell (Al)	70.5 GPa	2700 kg/m ³	0.30	350 mm	400	2 mm	55 mm

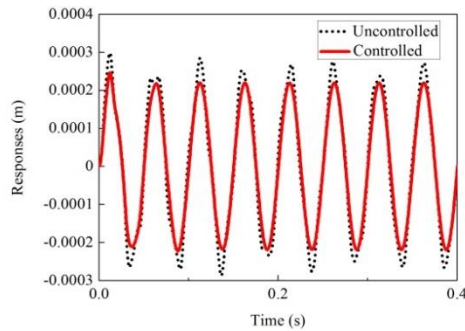


Fig. 3 time-history of the flat plate under 20 Hz sine excitation

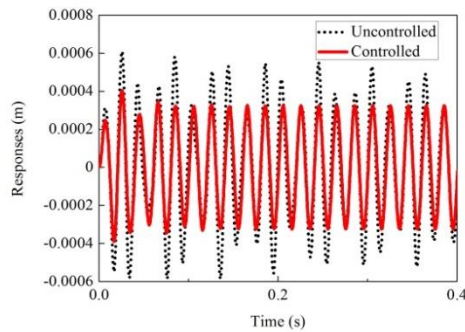


Fig. 4 time-history of the flat plate under 50 Hz sine excitation

Table 2 parameters of MFC

Model	Active Length	Active Width	Overall Length	Overall Width	Capacitance	Free Strain	Blocking Force
M8514-P1	85 mm	14 mm	101 mm	20 mm	3.39 nF	1600 ppm	202 N

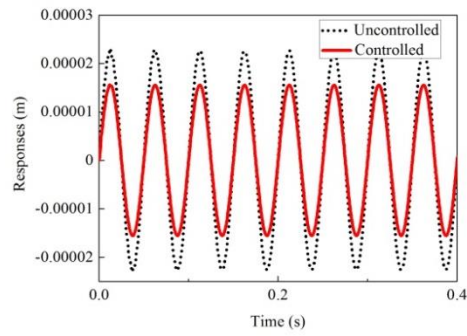


Fig. 5 time-history of the arc shell under 20 Hz sine excitation

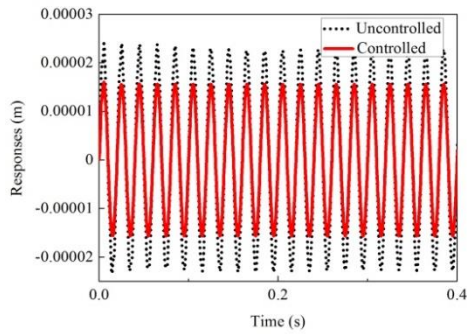


Fig. 6 time-history of the arc shell under 50 Hz sine excitation

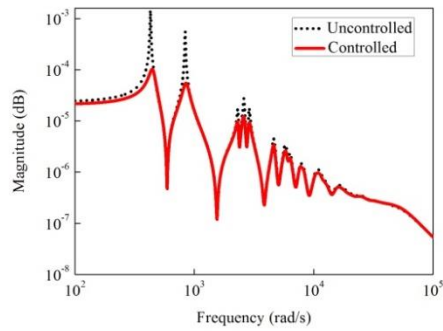


Fig. 7 frequency response of the flat plate

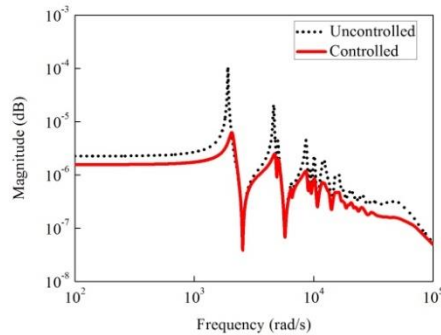


Fig. 8 frequency response of the arc shell

The time-history of flat plate and arc shell under sine load show that PID can reduce their vibration effectively. Under 20 Hz sine load, the maximum displacement of flat plate is reduced from 2.98×10^{-4} m to 2.41×10^{-4} m and that of arc shell from 2.30×10^{-5} m to 1.52×10^{-5} m; under 50 Hz sine load, the maximum displacement of flat plate is reduced from 6.10×10^{-4} m to 3.26×10^{-4} m and that of arc shell from 2.27×10^{-5} m to 1.56×10^{-5} m; the frequency response comparison shows that in the whole frequency band, PID control has a good control effect under most vibration frequency.

5. MFC active control experiment

To verify the established MFC actuation equation in this paper and the MFC vibration control effect on the plate and shell structure, the MFC active control experiment is conducted to the plate and shell structure, whose device is shown in Figs. 9 and 10. A vibration exciter, composed of signal source, power amplifier, and vibration source, is adopted under the structure. Above the plate, the ARF-A type of acceleration transducer is adopted to measure vibration response of the structure. The M8514-P1 type of MFC is attached to the plate to exert control force over vibration. The simple and practical PID control is used as the control algorithm.

The experiment process is: the signal source produces vibration signals which are amplified by the power amplifier to a needed force to be exerted to the structure and make it vibrate; the acceleration transducer measures the acceleration of the plate vibration; signals are input into dSPACE signal acquisition module through A/D conversion, obtaining voltage control signals through the control program compiled by dSPACE; then they are input into high voltage amplifier after D/A conversion; the voltage is input into MFC to produce controlling force to implement vibration control over the plate and shell structure.

Figs. 11 and 12 are acceleration time-history comparison before and after the control over the flat plate under 20 Hz and 50 Hz excitation frequency and 300 V control voltage. Figs. 13 and 14 are acceleration time-history comparison before and after the control over the arc shell under 20 Hz and 50 Hz excitation frequency and 300 V control voltage. It is shown that piezoelectric fiber composite material (MFC) can also reduce vibration of plate and shell effectively. Under two different excitation frequencies, PID control algorithm also has great control effect.

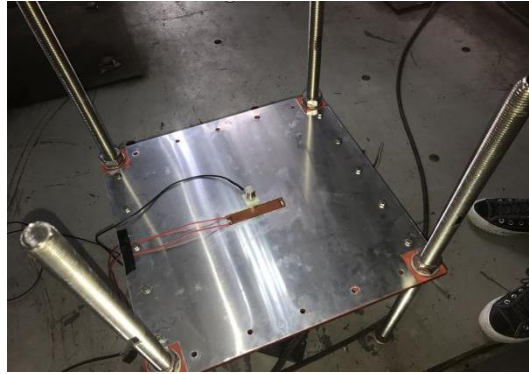


Fig. 9 the experimental model of the flat plate

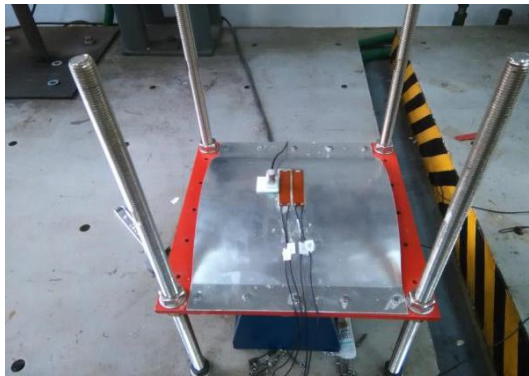


Fig. 10 the experimental model of the arc shell

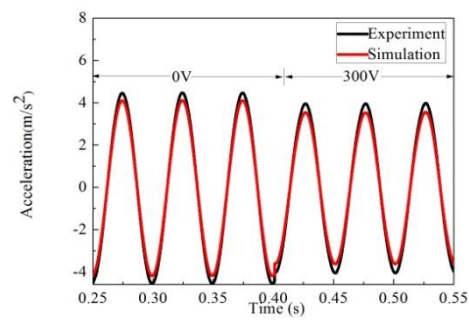


Fig. 11 acceleration time-history of the flat plate under 20HZ excitation

In the experiment of the flat plate, with 20 Hz exciting force and 300 V voltage, MFC can reduce the acceleration amplitude by 7%, while in simulation MFC can reduce it by 9%. In the experiment, with 50 Hz exciting force and 300 V voltage, MFC can reduce the acceleration amplitude by 13%, while in simulation MFC can reduce it by 16%.

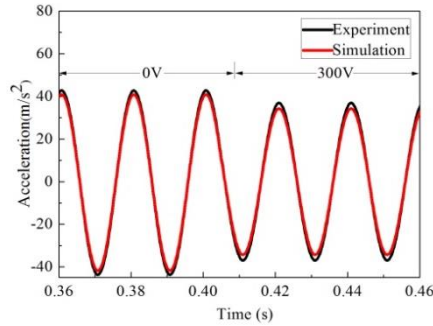


Fig. 12 acceleration time-history of the flat plate under 50 HZ excitation

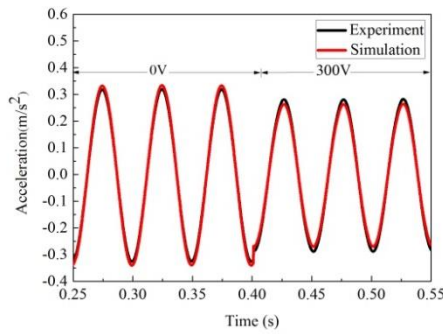


Fig. 13 acceleration time-history of the arc shell under 20 HZ excitation

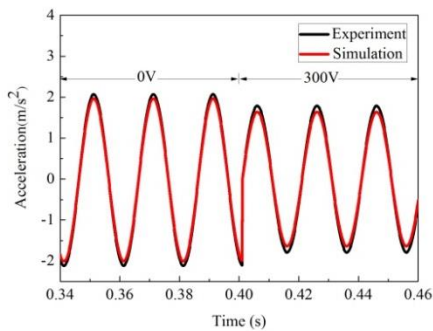


Fig. 14 acceleration time-history of the arc shell under 50 HZ excitation

In the experiment of the arc shell, with 20 Hz exciting force and 300 V voltage, MFC can reduce the acceleration amplitude by 9.54%, while in simulation MFC can reduce it by 21.12%. In the experiment, with 50 Hz exciting force and 300 V voltage, MFC can reduce the acceleration amplitude by 12.68%, while in simulation MFC can reduce it by 18.50%.

In the control experiment of plate and shell vibration, it is also found that the experimental curve and the simulation curve before and after control basically coincide with each other. In the experiment of the flat plate, with 20 Hz exciting force and 300 V voltage, the deviation between experimental and simulation acceleration amplitude before control is 8.06%, while that after control is 10.55%; with 50 Hz exciting force and 300 V voltage, the deviation between experimental and simulation acceleration amplitude before control is 4.56%, while that after control is 7.29%. In the experiment of the arc shell, with 20 Hz exciting force and 300 V voltage, the deviation between experimental and simulation acceleration amplitude before control is 4.50%, while that after control is 6.41%; with 50 Hz exciting force and 300 V voltage, the deviation between experimental and simulation acceleration amplitude before control is 5.18%, while that after control is 8.52%. This proves the correctness of the actuation equation deduced in this paper and the effectiveness of the modeling method based on finite element.

6. Conclusions

The plate and shell structure being the control object, this paper deduces the actuating force and bending moment formula of MFC coupled plate, considering the influence of internal force of the cross-section at MFC paste position under the binding boundary condition. The simulation and experiment of vibration control are conducted over flat plate and arc shell, obtaining the comparison results before and after control under 20Hz and 50Hz excitation. The deviation of acceleration amplitude of simulation and experiment between flat plate and arc shell is quite small and their curves highly coincide. The comparison results not only prove that the MFC actuation equation deduced in this paper is applicable, but indicate that MFC has great control effect on vibration of plate and shell structure.

Acknowledgments

The research described in this paper was financially supported by the National Natural Science Foundation of China, project No 51478372, Natural Science Foundation of Hubei Province, project No 2016CFA020 and the Fundamental Research Funds for the Central Universities, project No 2017-zy-055.

References

- Bilgen, O., Erturk, A. and Inman, D.J. (2010), "Analytical and experimental characterization of macro-fiber composite actuated thin clamped-free unimorph benders", *J. Vib. Acoust.*, **132**(5), 051005.
- Deraemaeker, A., Nasser, H., Benjeddou, A. and Preumont, A. (2009), "Mixing rules for the piezoelectric properties of macro fiber composites", *J. Intel. Mat. Syst. Str.*, **20**(12), 1475-1482.
- Kim, H.S., Sohn, J.S. and Choi, S.B. (2011), "Vibration control of a cylindrical shell structure using macro fiber composite actuators", *Mech. Based. Des. Struc.*, **39**(4), 491-506.
- Kumar, G.V., Raja, S., Prasanna, K.B. and Sudha V. (2012), "Finite element analysis and vibration control of a deep composite cylindrical shell using MFC actuators", *Smart Mater. Res.*, <http://dx.doi.org/10.1155/2012/513271>.
- Kwak, M.K., Heo, S. and Jeong, M. (2009), "Dynamic modeling and active vibration controller design for a

- cylindrical shell equipped with piezoelectric sensors and actuators”, *J. Sound Vib.*, **321**(3-5), 510-524.
- Ma, G., Xu, M., An, Z., Wu, C. and Miao, W. (2016), “Active vibration control of an axially moving cantilever structure using MFC”, *Int. J. Appl. Electrom.*, **52**(3), 967-974.
- Prasath, S.S. and Arockiarajan, A. (2013), “Effective electromechanical response of macro-fiber composite (MFC): analytical and numerical models”, *Int. J. Mech. Sci.*, **77**(77), 98-106.
- Prasath, S.S. and Arockiarajan, A. (2014), “Analytical, numerical and experimental predictions of the effective electromechanical properties of macro-fiber composite (MFC)”, *Sensor Actuat A-Phys.*, **214**(4), 31-44.
- Sohn, J.W. and Choi, S.B. (2014), “Active vibration control of a cylindrical structure using flexible piezoactuators: experimental work in air and water environments”, *Smart Mater. Struct.*, **23**(11), 117002(9pp).
- Steiger, K. and Mokrý, P. (2015), “Finite element analysis of the Macro Fiber Composite actuator: Macroscopic elastic and piezoelectric properties and active control thereof by means of negative capacitance shunt circuit”, *Smart Mater. Struct.*, **24**(2), 25-51.
- Williams, R.B., Park, G., Inman, D.J. and Wilkie, W.K. (2002), “An overview of composite actuators with piezoceramic fibers”, *Proceedings of the 20th International Modal Analysis Conference*, Los Angeles, United States, February.
- Yi, G., Liu, Y. and Leng, J. (2011), “Active vibration control of basic structures using macro fiber composites”, *Proceedings of SPIE - The International Society for Optical Engineering*, California, United States, March.
- Zhang, S.Q., Li Y.X. and Schmidt, R. (2015), “Modeling and simulation of macro-fiber composite layered smart structures”, *Compos. Struct.*, **126**, 89-100.
- Zhao, J., Man, X., Xue, X., Sun, Q. and Zhang, L. (2014), “Numerical research on electro-elastic properties of the macro fiber composite (MFC) actuators”, *Int. J. Appl. Electrom.*, **45** (1), 409-415.